JGR Atmospheres

RESEARCH ARTICLE
10.1029/2022JD037737

Seasonality of the QBO Impact on Equatorial Clouds

Aodhan Sweeney[1], Qiang Fu[1,2], Hamid A. Pahlavan[1,3], and Peter Haynes[2]

[1]Department of Atmospheric Sciences, University of Washington, Seattle, WA, USA, [2]Department of Applied Mathematics and Theoretical Physics, University of Cambridge, Cambridge, UK, [3]Department of Mechanical Engineering, Rice University, Houston, TX, USA

Key Points:

- The Quasi-Biennial Oscillation (QBO) significantly impacts high equatorial clouds during boreal spring and early summer
- QBO-related cloud changes result in a statistically significant change in the longwave cloud radiative effect by ~1 Wm^{-2}
- The seasonality of the QBO impact on clouds is synchronized with upper tropospheric intrusions of QBO related temperature and zonal wind

Supporting Information:

Supporting Information may be found in the online version of this article.

Correspondence to:

A. Sweeney,
aodhan@uw.edu

Citation:

Sweeney, A., Fu, Q., Pahlavan, H. A., & Haynes, P. (2023). Seasonality of the QBO impact on equatorial clouds. *Journal of Geophysical Research: Atmospheres*, *128*, e2022JD037737. https://doi.org/10.1029/2022JD037737

Received 29 AUG 2022
Accepted 10 MAR 2023

Abstract The Quasi-Biennial Oscillation (QBO) dominates the interannual variability in the tropical lower stratosphere and is characterized by the descent of alternating easterly and westerly zonal winds. The QBO impact on tropical clouds and convection has received great attention in recent years due to its implications for weather and climate. In this study, a 15-year record of high vertical resolution cloud observations from CALIPSO and a 50 hPa zonal wind QBO index from ERA5 are used to document the QBO impact on equatorial (10°S–10°N) clouds. Observations from radio occultations, the CERES instrument, and the ERA5 reanalysis are also used to document the QBO impact on temperature, cloud radiative effect (CRE), and zonal wind, respectively. It is shown that the QBO impact on zonal mean equatorial cloud fraction has a strong seasonality. The strongest cloud fraction response to the QBO occurs in boreal spring and early summer, which extends from above the mean tropopause to ~12.5 km and results in a significant longwave CRE anomaly of 1 W/m^2. The seasonality of the QBO impact on cloud fraction is synchronized with the QBO impacts on temperature and zonal wind in the tropical upper troposphere.

Plain Language Summary Approximately every 2 years, eastward or westward winds in the stratosphere above the equator reverse their direction. This pattern of alternating wind direction is called the Quasi-Biennial Oscillation (QBO). In this study, we use fine vertical resolution satellite data to examine the QBO impact on clouds, which can be signals of storminess and can impact weather and climate. We find that the QBO impact on equatorial clouds spans a deep vertical extent of the upper troposphere and shows a strong seasonality. These cloud responses imply a significant change in the Earth's radiation budget. We also find that the seasonal variations in QBO-cloud connections are concurrent with seasonal variation in QBO-related wind and temperature signals. These changes are most significant during northern hemisphere spring and early summer.

1. Introduction

The Quasi-Biennial Oscillation (QBO) is the main mode of variability in the tropical lower stratosphere and is characterized by descending regions of alternating zonal winds and temperature anomalies connected through thermal wind balance (Andrews et al., 1987; Baldwin et al., 2001; Fueglistaler & Haynes, 2005; Holton & Lindzen, 1972; Lindzen & Holton, 1968; Pahlavan, Fu, et al., 2021; Plumb & Bell, 1982). Although the QBO zonal wind amplitude decreases rapidly below 50 hPa (e.g., Match & Fueglistaler, 2019; Saravanan, 1990) the QBO has been shown to impact the troposphere. One important route of QBO influence on the extratropical troposphere is through the QBO modulation of the stratospheric polar vortex (Anstey & Shepherd, 2014; Baldwin et al., 2001; Holton and Tan, 1980, 1982; Lu et al., 2020). Another potentially more direct impact is on the tropical troposphere through the QBO modulation of tropical clouds and convection (Collimore et al., 2003; Haynes et al., 2021; Hitchman et al., 2021; Liess & Geller, 2012; Son et al., 2017; Tseng & Fu, 2017a). It has been suggested that the impact of the QBO on tropical clouds and convection may work by modulating the thermodynamic (temperature and static stability) and dynamic (vertical wind shear) properties of the transition layer between the tropical troposphere and stratosphere (Collimore et al., 2003; Garcia-Franco et al., 2022; Giorgetta et al., 1999; Gray et al., 2018; Haynes et al., 2021; Jaramillo et al., 2021; Martin et al., 2019; Tseng & Fu, 2017a). This layer is called the tropical tropopause layer (TTL) and extends from ~14.5 to 18.5 km (Fu et al., 2007; Fueglistalaer et al., 2009).

Interest in the QBO direct impact on the tropical troposphere has recently been invigorated due to the correlation between the Madden-Julian Oscillation (MJO) and the QBO (Lin & Emanuel, 2022; Martin, Son, et al., 2021; Son et al., 2017; Yoo & Son, 2016; Zhang & Zhang, 2018). Many attempts to explain the connection focus on

the anomalously cold TTL temperatures, decreased TTL static stability, and increased TTL cirrus clouds when the QBO is easterly near 50 hPa (e.g., Densmore et al., 2019; Hendon & Abhik, 2018; Klotzbach et al., 2019; Sakaeda et al., 2020; Son et al., 2017). Curiously, the QBO-MJO connection has been shown to be only present in boreal winter (e.g., Yoo & Son, 2016), while QBO impacts on tropical convection have also been found during other seasons (Collimore et al., 2003; Densmore et al., 2019; Giorgetta et al., 1999; Gray et al., 2018). Studies also show that the QBO impact on the thermodynamic and dynamic properties of the TTL varies strongly across seasons (Hitchman et al., 2021; Martin, Sobel, et al., 2021; Sakaeda et al., 2020; Tegtmeier et al., 2020). To explain these variations, these studies have tended to focus on the seasonal variation in the troposphere without regard to potential systematic seasonal variation in the QBO above the tropopause (Son et al., 2017; Tegtmeier et al., 2020). In fact, it has been shown that the QBO itself undergoes strong seasonality, showing seasonal variations in the QBO acceleration near 50 and 70 hPa (Coy et al., 2020; Dunkerton, 1990). This may be due to the seasonality of the QBO wave forcing at these levels (Maruyama, 1991; Sjoberg et al., 2017; Tindall et al., 2006) or by the Brewer-Dobson Circulation (BDC) which potentially affects QBO descent rate throughout much of the stratosphere (Coy et al., 2020; Hampson & Haynes, 2004; Kinnersley & Pawson, 1996; Mote et al., 1996; Rajendran et al., 2018). Whether these seasonal QBO variations are important for the QBO's direct impact on the troposphere is still not known.

Previous investigations of the QBO direct impact on the tropical troposphere showed anomalies in temperature, zonal wind, clouds, deep convection, and even Outgoing Longwave Radiation (e.g., Collimore et al., 2003; Huesmann & Hitchman, 2001). Interpretations of these results were limited by the poor vertical resolution of reanalysis, strong zonal and seasonal variations, and inconsistent QBO definitions. More recent work using improved reanalysis products and precipitation data has confirmed the strong longitudinal and seasonal variation in the tropical tropospheric QBO signal (e.g., Gray et al., 2018; Liess & Geller, 2012). These longitudinal and seasonal asymmetries complicate analysis of the QBO direct impact and the physical mechanisms responsible.

An important component of the QBO direct impact is its effect on high altitude cirrus clouds which can heat the troposphere but cool the stratosphere (Fu et al., 2018; Fueglistaler & Fu, 2006), decreasing the stability of the TTL. These clouds have also been suggested as a potentially important modulator of the QBO-MJO connection (e.g., Lin & Emanuel, 2022; Martin, Son, et al., 2021; Son et al., 2017). Apart from these potential couplings, high altitude cirrus clouds are also important because of their impact on the TTL radiative heating rate, troposphere-stratosphere transport, and TTL thermal structure (Corti et al., 2005, 2006; Davis et al., 2013; Dessler et al., 2013; Flury et al., 2012; Fu et al., 2018; Hartmann et al., 2001; Hong et al., 2016; Tseng & Fu, 2017a; Wang & Fu, 2021; Yang et al., 2010). These cirrus clouds also exhibit a greenhouse effect, thus impacting the CRE which can change the energy budget of the tropics.

Accurate documentation of the QBO direct impact requires high vertical resolution observations in the TTL, where communication between the tropical stratosphere and troposphere takes place. This study documents the seasonality of the QBO vertical impact on equatorial high clouds using high vertical resolution CALIPSO lidar data. Temperature and radiative energy budget observations are obtained independently from GPSRO- and CERES instruments. The QBO response in zonal wind is analyzed using ERA5 reanalysis data. This study focuses primarily on the zonal mean QBO impact to simplify complications due to zonal asymmetries. Unique to this study is the documentation of the QBO impact on vertical profiles of clouds and temperature as it descends from the lower stratosphere into the TTL for various seasons. We find that the QBO impact on clouds undergoes large seasonal variations reaching its maximum depth in boreal spring and early summer 3 months after the QBO-related zonal wind has maximized at the 50 hPa level. These deep cloud fraction anomalies extend from above the tropopause to as low as ∼12.5 km (∼180 hPa) and are synchronized with tropospheric intrusions of QBO related temperature and zonal wind anomalies in the TTL. Deep cloud fraction anomalies are concurrent with a statistically significant QBO impact on the equatorial longwave CRE. Section 2 describes information about the data and methods used in this study, Section 3 shows the results, and Section 4 provides the potential causes and implications of these results.

2. Data and Methods

2.1. Satellite Observations and ERA5 Reanalysis

2.1.1. CALIPSO Cloud Observations

The CALIPSO satellite was launched in April 2006 into a sun synchronous orbit with local equatorial crossing times at 01:30 and 13:30 (Winker et al., 2010). The main instrument used in this study is the Cloud-Aerosol Lidar with Orthogonal Polarization (CALIOP) dual wavelength polarization sensitive lidar. CALIOP can provide information of cloud layers with optical depth from ∼0.01 to ∼4 at which the CALIOP signal becomes fully attenuated. In this study we use the Level 2 V4.2 5-km Merged Layer Product with a vertical resolution of 60 m from June of 2006 to December of 2020. The primary quantity used from the CALIPSO data is the cloud fraction above 11 km, which is defined as the number of detections of clouds divided by the total number of observations in each 2.5° × 2.5° grid cell.

Previous versions of the CALIOP data did not identify clouds above the lapse rate tropopause, potentially missing a large amount of TTL cirrus clouds (Tseng & Fu, 2017b). The recent V4 release of CALIOP data has improved detection of TTL cirrus by applying the cloud-aerosol distinction algorithm to layers above the lapse-rate tropopause. With these V4 changes, we find significant amounts of stratospheric aerosols that are misidentified as TTL cirrus clouds. These stratospheric aerosols appear to be directly linked to tropical volcanic eruptions (Tseng & Fu, 2017b). Tseng and Fu (2017b) found that previous versions of the Level 2 data could be used to accurately identify TTL cirrus clouds above the lapse rate tropopause by using the volume depolarization ratio (VDR). We similarly apply this VDR threshold of VDR > 0.12 for all layers identified above the lapse-rate tropopause. This largely eliminates the amount of falsely identified TTL cirrus clouds in February–April of 2014, which corresponds to the 2014 Kelud eruption in Indonesia.

2.1.2. Global Positioning System-Radio Occultation Temperature Observations

Temperature profile data comes from Global Positioning System-Radio Occultation (GPS-RO) receivers onboard the COSMIC-1, MetOp-A and MetOp-B satellites which are archived at the University Corporation for Atmospheric Research (UCAR) (Sweeney & Fu, 2021). We use GPS-RO data from June of 2006 to December of 2020. Radio occultations are retrieved using an active limb sounding technique, allowing for retrieval of bending angle and refractivity, which can be used to derive temperature (Kursinski et al., 1997). GPS-RO temperature profiles have low error (less than 0.1 K), as well as high vertical resolution (∼0.5 km) in the tropical upper troposphere, and lower stratosphere but relatively coarse horizontal resolution (about 200 km) (Kuo et al., 2004; Kursinski et al., 1997; Zeng et al., 2019). We use the level-2 wetPrf product (Sweeney & Fu, 2021), which provides estimates of temperature including the effects of moisture and is equivalent to the dry profiles when humidity is negligible (as it is in the TTL) (Kursinski et al., 1997).

2.1.3. CERES Observations and ERA5 Reanalysis

To quantify the QBO impact on the CRE at the top of the atmosphere, we use the level three CERES Energy Balance and Filled Climate Data Record (Loeb et al., 2018). Data used from this record spans 2006–2020 and is provided at 1° × 1° horizontal resolution. CERES observations include the "all sky" and "clear sky" components of the longwave radiation fluxes at the top of the atmosphere. Taking the difference between these provides the CRE on longwave radiation. The ERA5 reanalysis is used to create the QBO index, analyze the QBO impacts on zonal wind, and diagnose the zonal wind tendencies. The QBO index and analysis of QBO zonal winds is done using monthly mean ERA5 data with 1° × 1° horizontal resolution. The zonal wind tendency analysis is completed using 1° × 1° horizontal resolution with 6-hourly temporal resolution.

2.2. QBO Index and Analysis Method

The QBO index is the 10°S–10°N 50 hPa zonal mean zonal wind anomalies taken from the ERA5 reanalysis (Hersbach et al., 2020; Martin, Sobel, et al., 2021; Pahlavan, Fu, et al., 2021). As is well-known, the phase of the QBO varies strongly with height. Correlations of QBO winds with other variables will therefore depend strongly on the height at which the wind is measured. One approach has been to use an emperical orthogonal function representation of the QBO (Wallace et al., 1993), however this has the disadvantage that the phase is determined by combining information from many levels, which may not be optimal when considering variations in the lower

stratosphere. The approach here is to use 50 hPa winds, but to consider different lagged correlation with these winds (e.g., Ding & Fu, 2018; Liess & Geller, 2012; Tseng & Fu, 2017a). The 50 hPa (∼21 km) level sits above the TTL. Assuming the QBO descent rate is ∼1 km/month, then using the QBO index at 50 hPa with leads from zero to 4 months will allow for assessment of the QBO impact as it descends into the TTL. Results regarding cloud fraction are recreated using QBO indices based on both 70 and 30 hPa zonal winds with similar conclusions (see Figures S1 and S2 in Supporting Information S1).

Satellite observations and the ERA5 reanalysis data are used to document the impact of the QBO on equatorial cloud fraction, temperature, zonal wind, and radiative energy budget. To focus on the interannual variability caused by the QBO, the seasonal cycle is first removed from all variables. Anomalies to the seasonal cycle are denoted in figures and throughout the text using the notation X' where X is a given variable of interest and ' denotes the anomaly after removing the seasonal cycle. This study isolates the QBO impact by averaging months of data where the 50 hPa zonal wind is above and below ±0.5 standard deviations from the mean, corresponding to QBO westerly (QBOW) and easterly (QBOE) components respectively (e.g., Martin, Sobel, et al., 2021; Son et al., 2017; Yoo & Son, 2016). Note that "impact" throughout the text refers to the QBO signal in each variable X after constructing the QBOW-QBOE composite and is not necessarily meant to imply causality. To reduce the effect of month-to-month variability, we analyze the seasonality of the QBO impact using composites created using three consecutive months instead of each month individually. Significance of the difference composites between QBOW and QBOE is tested using a Welch's t test with a significance threshold of 95%. The analysis was repeated using the regression approach and statistical significance was tested accounting for autocorrelation leading to similar results (not shown). To reduce the potential aliasing of any El-Nino signal in the composites created, the ENSO 3.4 signal is regressed out of all fields before creating the figures. Our sensitivity tests indicate that removing the ENSO signal has very little effect on the derived zonal mean QBO response in all variables, and a weak (but slightly larger) effect on the derived zonal distribution response to the QBO.

3. Results

3.1. Zonal Mean Cloud Fraction

Figure 1 shows the impact of the QBO on equatorial cloud fraction using the QBOW-QBOE cloud fraction composites. Each panel represents cloud fraction response as a function of season and height from ∼11 to 20 km. Columns represent months of lead used for the QBO index. For example, the cloud anomalies at AMJ in the fourth column (3 Month Lead) are related to the 50 hPa QBO index in JFM. Rows show the partitioning of different cloud types. The first row shows the QBO response in cloud fraction considering all clouds, called All Cloud fraction. The All Cloud fractions are further divided into three subtypes. The TTL Cirrus (second row in Figure 1) are clouds with bases above 14.5 km (Tseng & Fu, 2017a). The Opaque Clouds (fourth row in Figure 1) are the cloud layers where the lidar signal becomes saturated, which are often associated with deep convection and thick anvil. Because the Opaque Clouds saturate the lidar, no clouds below are detectible so we assume that all layers below the opaque cloud levels are also cloudy layers. Other Cirrus (third row in Figure 1) are clouds that are not TTL Cirrus or Opaque Clouds, which are associated with thin anvil and cirrus clouds that have bases below 14.5 km (Sokol & Hartmann, 2020). In all plots, the thick black line represents the cold point tropopause (CPT) height from the GPS-RO data, and the stippling indicates regions where results are statistically significant.

All significant cloud fraction changes are negative. This is consistent with the idea that the warmer temperatures associated with QBOW decrease cloud fraction, whereas the opposite is true for QBOE. All Cloud fraction changes (first row of Figure 1) maximize below the tropopause, and a large seasonality in magnitude is evident regardless of lead time chosen. The largest All Cloud fraction impacts occur below the tropopause level using a 1-month lead of the QBO index from JFM-MJJ and from SON-NDJ, reaching a maximum magnitude of up to 8%. The weakest response at this level is in JAS and may be caused by the weak QBO-related temperature anomalies (Hitchman et al., 2021; Martin, Sobel, et al., 2021; Sakaeda et al., 2020) and small climatological cloud amount (Tseng & Fu, 2017b) during these months. A much weaker local minimum also occurs in DJF.

In addition to the magnitude of the cloud fraction responses, the vertical extent (i.e., thickness of the cloud fraction change) is also sensitive to lead time and season. The vertical extent of the statistically significant region using a 0-month lead is roughly constant across seasons but appears to be slightly smaller in JAS and DJF. Using a 2-month lead, a vertically extensive maximum near MAM-AMJ becomes more apparent, and statistically

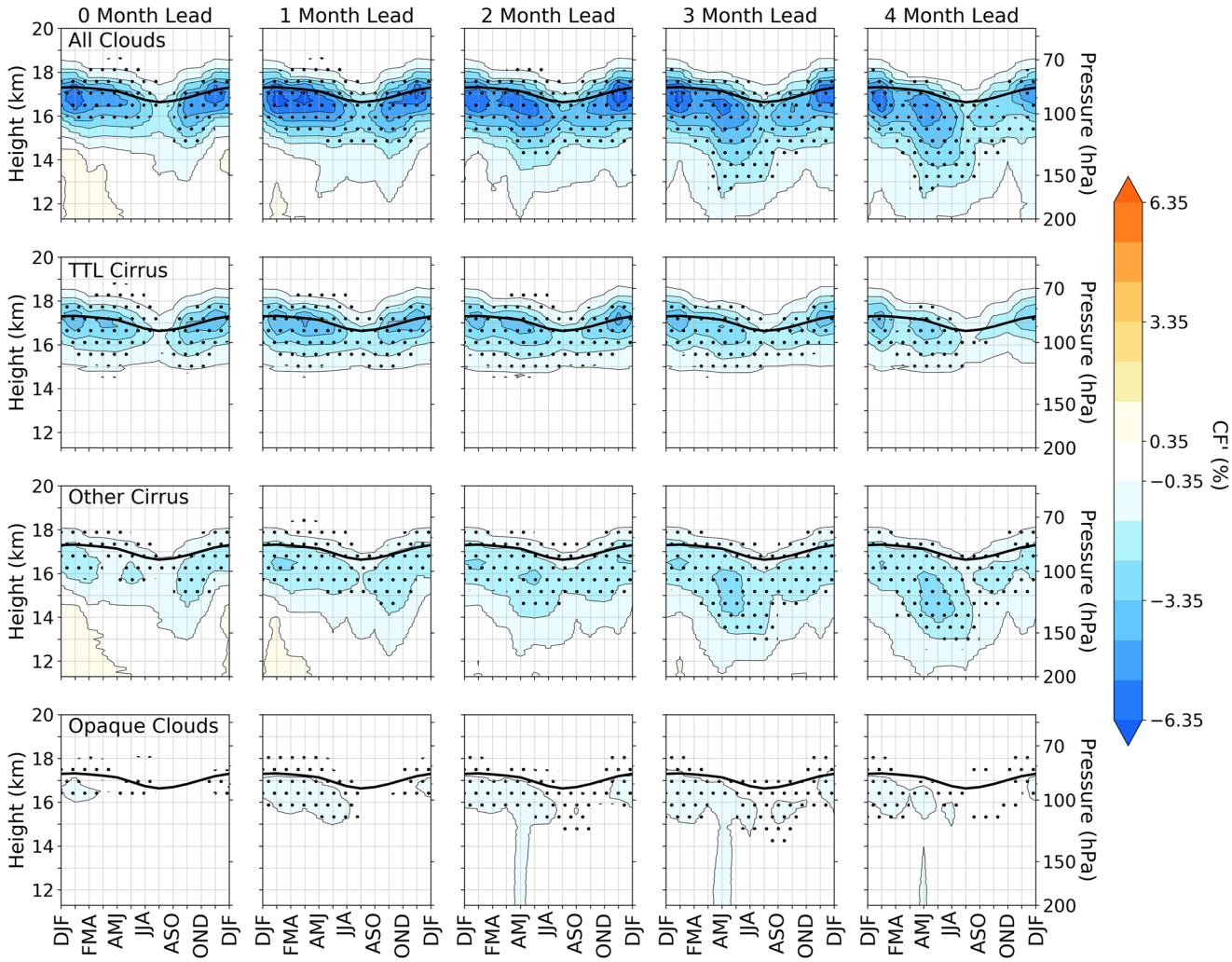

Figure 1. Seasonality of zonal-mean QBOW-QBOE anomaly composites averaged over 10°S–10°N as a function of height for All Cloud fractions (first row), which are further divided into tropical tropopause layer Cirrus (second row), Other Cirrus (third row), and Opaque Clouds (fourth row). The columns represent various leads of the Quasi-Biennial Oscillation index used. Thick black lines show the mean cold point tropopause. Stippling indicates regions where impact is significant at a **95**% confidence.

significant changes at this time are observed below 14 km. Using a 3-month lead, significant cloud fraction responses are observed as low as 12.5 km. These deep cloud fraction changes are only associated with the boreal spring and early summer. This deep cloud fraction change in boreal spring and summer can be reproduced using QBO indices defined at the 30 or 70 hPa levels, but with the maximum impact occurring at different lead times (see Figures S1 and S2 in Supporting Information S1).

Partitioning All Cloud fraction into its constituent groups reveals that the largest contributor to the changes in All Cloud fraction in the TTL are TTL Cirrus (second row in Figure 1). Many studies have shown that the QBO can impact the interannual variability of TTL Cirrus (e.g., Davis et al., 2013; Flury et al., 2012; Tseng & Fu, 2017a). The TTL Cirrus response reaches its maximum of ∼4.5% in JFM-MAM when using a 1-month lead of the QBO index. TTL Cirrus changes also undergo strong seasonality in their magnitude and vertical extent. The minimum vertical extent is observed in JAS, and a much weaker secondary minimum is observed in DJF which is most evident at lead times of two and less months. In the TTL, QBO related changes in the Other Cirrus (third row in Figure 1) are weaker than changes seen in the TTL Cirrus but much more vertically extensive because they do not have the 14.5 km cloud base threshold. Other Cirrus changes extend from above the tropopause to below the TTL, which is largely responsible for the significant deep intrusion of All Cloud fraction changes at a 3-month lead during boreal spring and summer. The fourth row of Figure 1 shows changes in Opaque Clouds. Zonal mean

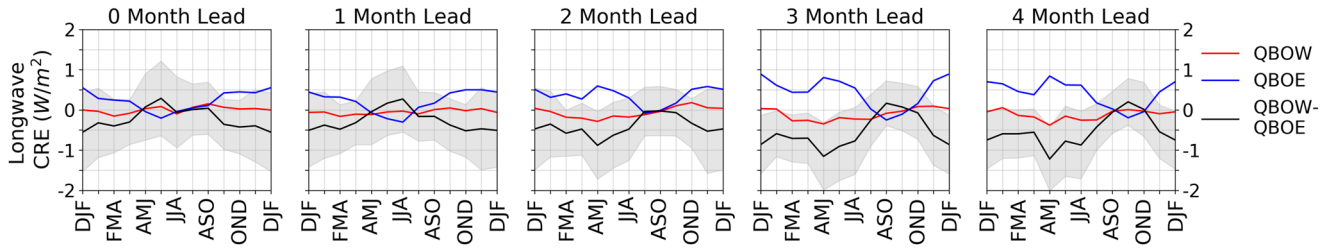

Figure 2. Seasonality of the Quasi-Biennial Oscillation (QBO) impact on longwave cloud radiative effect averaged over 10°S–10°N. The black line is the QBOW (red line) composite minus the QBOE (blue line) composite. The columns represent various leads of the QBO index. The shaded region shows the 2σ confidence intervals.

Opaque Cloud responses are weak but are still more apparent from JFM to MJJ when using QBO leads of between one and 3 months. Figure 1 shows that the QBO impact on zonal mean equatorial cloud fraction is sensitive to both the season and lead time chosen. Additionally, TTL Cirrus clouds and Other Cirrus clouds show peak response to the QBO in different seasons. The high magnitude and vertically extensive changes in cloud fraction raise the question of whether these cloud changes lead to significant changes in the radiative energy budget.

Figure 2 shows the longwave CRE as a function of lead time and season. The longwave CRE is derived from the independent CERES observations. The red (blue) line in Figure 2 shows the composite longwave CRE' for QBOW (QBOE) and the black line shows QBOW-QBOE. Gray shading around the QBOW-QBOE composite shows the 2σ confidence interval, coming from a 1,000 iteration bootstrap. Cirrus clouds have a greenhouse effect and thus a positive longwave CRE. Decreases in high cloud fraction observed in Figure 1 should be associated with decreases in the longwave CRE (see black line in Figure 2). The observed changes in the CRE' (black line in Figure 2) are largely consistent with observed changes in cloud fraction (Figure 1). The largest statistically significant longwave CRE decrease in response to QBO is observed during boreal spring and summer when using QBO leads of 3 and 4 months, which is ∼1 W/m^2. The AMJ longwave monthly CRE anomalies range from ±3.5 W/m^2 with a standard deviation of 1.23 W/m^2. Using the 50 hPa QBO index with a lead of 3 months, the correlation between the QBO and AMJ longwave CRE monthly anomalies is 0.44, which explains ∼20% of this season's longwave CRE variance.

This change in longwave CRE is synchronized with the deep changes in cloud fraction observed in Figure 1. This result lays out a potential connection between the QBO and the radiative energy budget through the impact on clouds.

The QBOE in Figure 2 (blue line) generally shows increases in the longwave CRE' as expected. Notably, QBOW (red line) shows little to no CRE' changes. Comparisons of the individual QBOW and QBOE composites of All Clouds in Figure 3a reveal that QBOE anomalies have larger magnitude and are deeper, extending to below 14 km. Figure 3b shows regression coefficients of the LW CRE regressed onto All Cloud fraction, indicating that

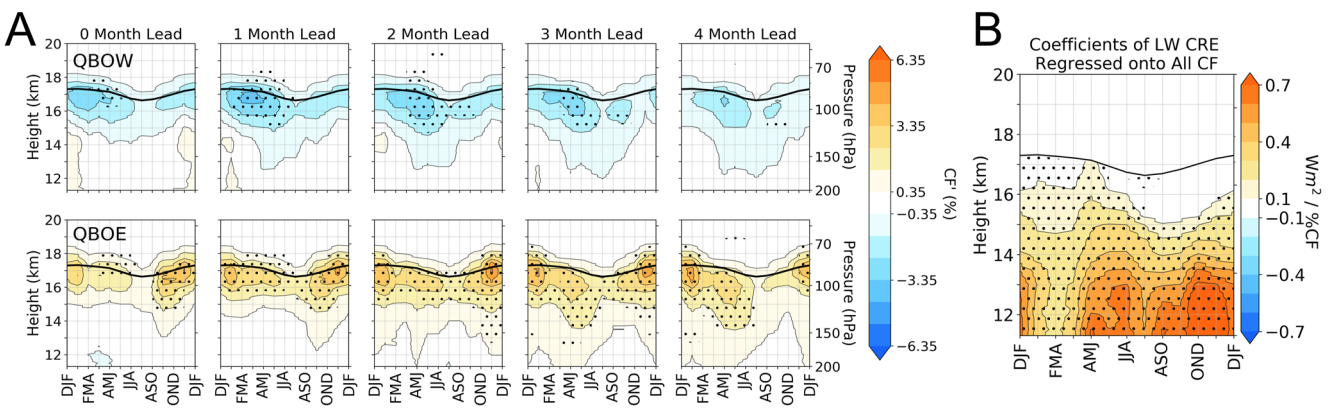

Figure 3. (a) All Cloud fraction composites based the Quasi-Biennial Oscillation (QBO) westerly (top) and QBO easterly (bottom) phases. The columns, thick black lines, and stippling are the same as in Figure 1. The difference between the QBOW and QBOE is shown in the first row of Figure 1 (b) Regression coefficients of the longwave cloud radiative effect regressed onto All Cloud fraction.

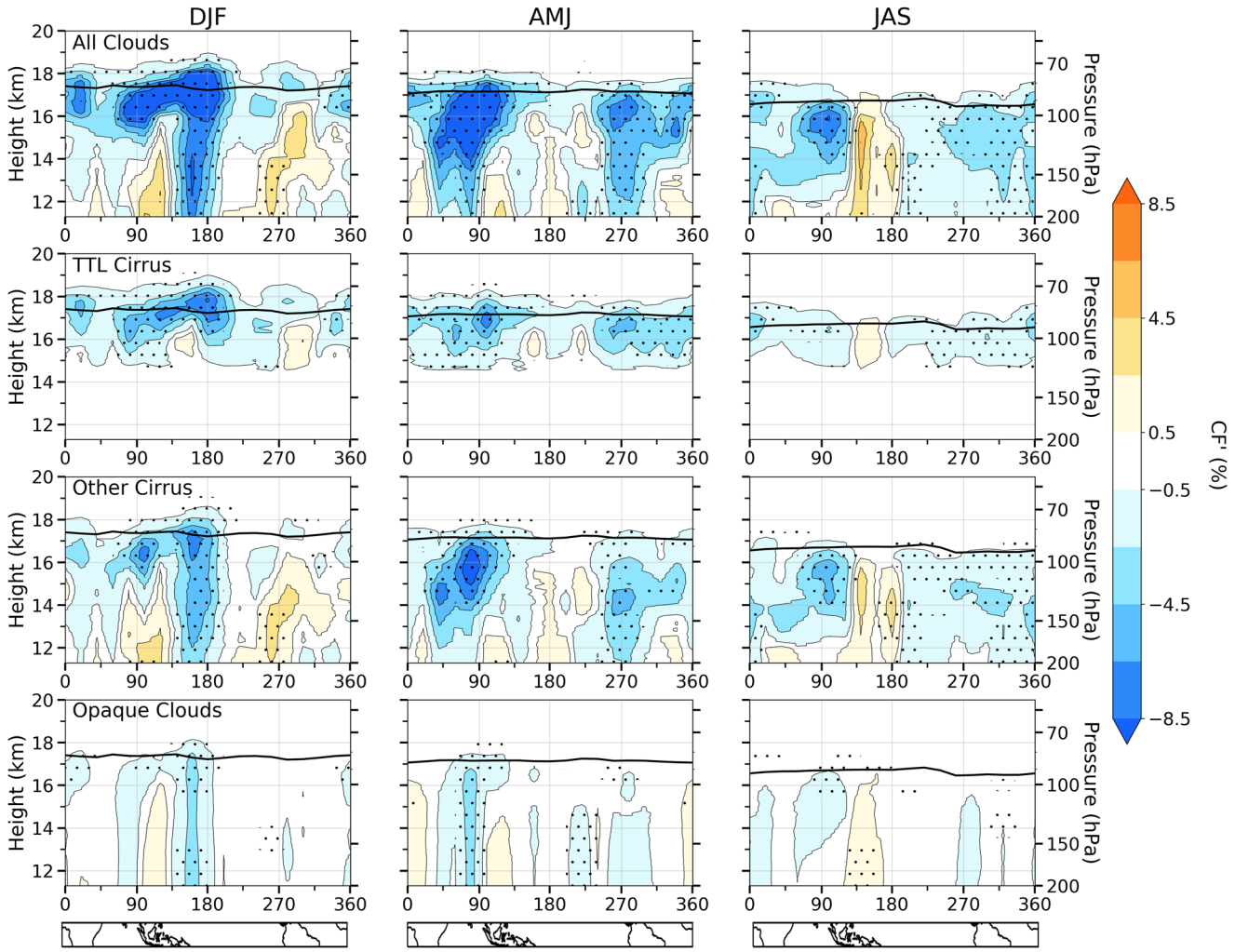

Figure 4. Zonal distribution of QBOW-QBOE anomaly composites averaged over 10°S–10°N as a function of height for All Cloud fractions (first row), tropical tropopause layer Cirrus (second row), Other Cirrus (third row), and Opaque Clouds (fourth row), in DJF (column 1), AMJ (column 2), and JAS (column 3) seasons. The Quasi-Biennial Oscillation lead is 3 months. Thick black lines show the tropopause. Stippling regions indicate that anomaly is significant at a 95% confidence interval. Continental outlines of the 10°S–10°N region are provided below each column.

cloud fraction perturbations lower in the atmosphere tend to have larger CRE impacts than those near the tropopause. Physically, this is because clouds near the tropopause are optically thin TTL Cirrus clouds. Lower in the atmosphere the clouds are optically thicker and contribute more strongly to the CRE. The QBOW only impacts the highest cirrus clouds, which have little effect on the longwave CRE. It is because of the deeper cloud fraction impacts associated with QBOE that is responsible for most of the CRE impact in Figure 2.

Previous studies have suggested the QBO impact on the TTL is zonally asymmetric and depends on longitude (Collimore et al., 2003; Ding & Fu, 2018; Son et al., 2017; Tegtmeier et al., 2020). Figure 4 provides the zonal structure of cloud fraction response to the QBO averaged over 10°S–10°N. For brevity, we only show QBOW-QBOE composites for a 3-month QBO lead in DJF, AMJ, and JAS seasons. Like all figures shown, the ENSO 3.4 signal was first regressed out before deriving the QBO composites. Continental outlines from 10°S to 10°N are provided at the bottom of each column. DJF, AMJ, and JAS are selected because of the previously suggested QBO-MJO connection season (DJF), and maximum (AMJ) and minimum (JAS) zonal All Cloud fraction response seasons (Figure 1). A climatology of zonal cloud fraction for these three seasons is provided in the Figure S3 in Supporting Information S1. Taking zonal averages of the fields in Figure 4 corresponds with the relevant month ranges in the 3-month lead column of Figure 1. All cloud fraction changes in both DJF and AMJ reach magnitudes of ∼10% but have different zonal structures leading to larger zonal mean cloud fraction anomalies in AMJ.

Negative changes over the Indian Ocean and those over the eastern Pacific in AMJ enforce each other, while during DJF the positive changes over the eastern Pacific partly cancel the negative ones over the western Pacific. The east-west contrast in the QBO signal in DJF is consistent with QBO-associated changes in the Walker circulation in boreal winter, which is associated with a relative reduction in precipitation in the western Pacific and increase in the eastern Pacific during QBOW compared to QBOE (Liess & Geller, 2012; Yamazaki et al., 2020).

In the TTL DJF All Cloud fraction shows a strong reduction that is eastward tilting with height and extends from the Indian Ocean to the western Pacific. These features are also present during DJF in the TTL Cirrus and Other Cirrus anomalies. The vertically eastward tilting portion of the cirrus structure is reminiscent of the vertically propagating Kelvin wave driven by tropical convection (Hendon & Abhik, 2018; Lim & Son, 2022; Virts et al., 2010; Virts & Wallace, 2014). This feature may be related to a QBO modulation of cirrus clouds associated with Kelvin waves in the TTL. TTL Cirrus fraction anomalies in AMJ show a weaker cirrus deck tilt, but All Cloud fraction responses over the Indian Ocean have the same sign all the way down due to the vertically extensive signature of both Other Cirrus and Opaque Clouds. The largest Opaque Cloud anomalies are found in DJF over the western Pacific and in AMJ over the Indian Ocean, consistent with the regions of deep intrusions of Other Cirrus cloud fraction response. Opposite to results of DJF, significant positive Opaque Cloud responses are found over the western Pacific in JAS (Collimore et al., 2003; Gray et al., 2018).

The height-longitude structure of the QBO response in clouds shown in Figure 4 may be compared with the corresponding structure of the climatological cloud fraction fields shown in Figure S3 in Supporting Information S1. Not surprisingly, the larger magnitude anomalies tend to be associated with the regions where cloud fraction is larger in the climatology. Maximum QBO-related cloud responses are typically above the climatological cloud maxima. Longitudinal variations of the cloud response are typically on the eastern and western flanks of climatological maxima in DJF and AMJ, respectively. Thus, in some cases, the QBOW-QBOE changes can be interpreted as a longitudinal shift in the cloudiness. However, the direction of this shift is not always the same and is sometimes eastward (e.g., DJF in the western Pacific) and sometimes westward (e.g., AMJ in the Indian Ocean). More straightforward is the reduction in cloud fraction in the TTL for the QBOW-QBOE composite.

3.2. Temperature and Zonal Wind in the TTL

Previous studies have shown that the variability of tropical high cloud fraction is frequently linked to changes in temperature and vertical temperature gradient (Kim et al., 2016; Tseng & Fu, 2017a; Chang & L'Ecuyer, 2020). The QBO may modulate the interannual variability of these clouds by changing the thermodynamic properties of the TTL (Davis et al., 2013; Flury et al., 2012; Tseng & Fu, 2017a). In this section, we investigate the QBO influence on the thermodynamic properties of the TTL. Figure 5 shows the responses of zonal-mean temperature anomalies (T') and vertical temperature gradient anomalies (dT'/dz) to the QBO as a function of season, height, and lead of the QBO index.

Using a zero-month lead, T' shows a large seasonal variation in the QBOW-QBOE amplitude above ∼18 km with peak magnitudes near 3.5 K in boreal winter. These results agree well with recent work showing that QBO-related lower-stratospheric and CPT temperature changes tend to be largest in boreal winter (Hitchman et al., 2021; Martin, Sobel, et al., 2021; Sakaeda et al., 2020; Tegtmeier et al., 2020). Boreal winter is also when TTL temperatures are lowest due to the stronger tropical upwelling associated with the BDC. Potential implications of this are discussed in Section 4. The seasonality of QBO related T' above the tropopause matches that of vertical wind shear between 50 and 70 hPa (not shown). Although the QBO T' response is large above the tropopause, below the tropopause there is little impact in both zero- and one-month leads. However, using leads of two or more months reveals temperature intrusions which penetrate the troposphere reaching their maximum depth of 14.5 km. Importantly, this deep temperature intrusion is only evident during boreal spring and summer. The second row of Figure 5 shows QBOW-QBOE composites in the vertical temperature gradient. Like the temperature intrusions observed in the first row, the changes of vertical temperature gradient also exhibit tropospheric penetration with a seasonal preference of boreal spring and summer.

The first row of Figure 5 shows that zonal mean QBO temperature perturbations can penetrate to lower altitudes during boreal spring and summer when considering the QBO with a lead of 3–4 months. The seasonal cycle of vertical wind shear in the 70–150 hPa region was compared to that of T' below the tropopause. Unlike the T' above the tropopause, whose seasonality matches that of the vertical wind shear, below tropopause T' responses

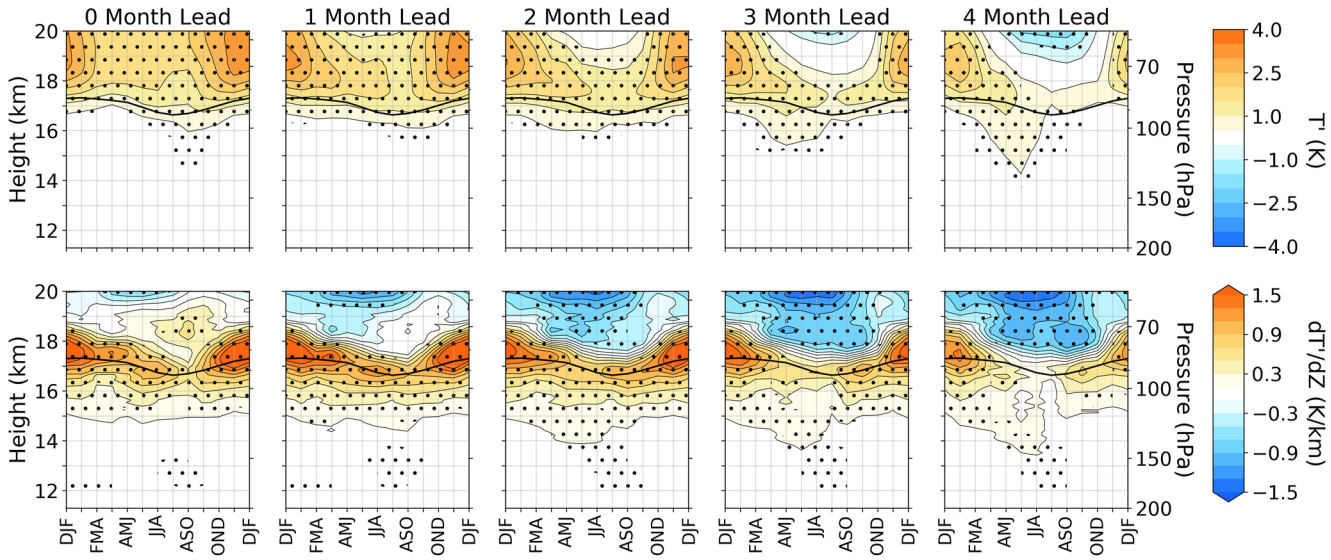

Figure 5. Seasonality of zonal-mean QBOW-QBOE anomaly composites averaged over 10°S–10°N as a function of height for temperature (first row) and vertical temperature gradients (second row). The columns, thick black lines, and stippling are the same as in Figure 1.

to the QBO do not share the same seasonality with vertical wind shear (not shown). This is likely because the seasonality of the QBO signal 70–150 hPa wind shear is too small to be isolated from the larger variability associated with tropospheric processes. Regardless of why these T' responses penetrate into the troposphere; it remains to be explained why they only occur in boreal spring and summer.

Fundamentally, the QBO is characterized by changes in the zonal mean zonal wind. Figure 6 shows QBOW-QBOE composites of zonal-mean zonal wind anomalies (U') in the TTL region. It reveals a large U' response above 19 km that reaches amplitudes of greater than 15 m/s. Using a 0-month lead, the 20 km U' exhibits little seasonality. At greater leads, the 20 km U' seasonality grows in a way analogous to temperature anomalies shown in Figure 5, as expected from the relation between temperatures and winds implied by thermal wind balance. From boreal spring to autumn the wind anomaly decays much faster with lead time than in boreal winter. In a modeling study, a similar faster decay of QBO jets near 50 hPa in boreal summer was attributed partially to the seasonal cycle of wave driving of the lower-stratospheric QBO jet and partially to the annual minimum in vertical velocity throughout the lower stratosphere during boreal summer (Krismer et al., 2013). When using leads of two to 4 months the zonal wind seasonality below the tropopause becomes more obvious. Deep intrusions of QBO-related zonal wind anomalies can reach as low as 15 km. Much like the anomalies seen for clouds (Figure 1), temperature, and vertical temperature gradient (Figure 5), these deep intrusions of zonal wind anomalies are only visible during boreal spring and summer (peak impact during MJJ). These zonal wind intrusions into the troposphere may be important for the general circulation of the upper troposphere, convective organization, and wave filtering of vertically propagating atmospheric waves (Baldwin et al., 2001; Collimore et al., 2003; Lane, 2021). Near 14 km and at leads of zero to 2 months a weak but statistically significant region of zonal wind anomalies

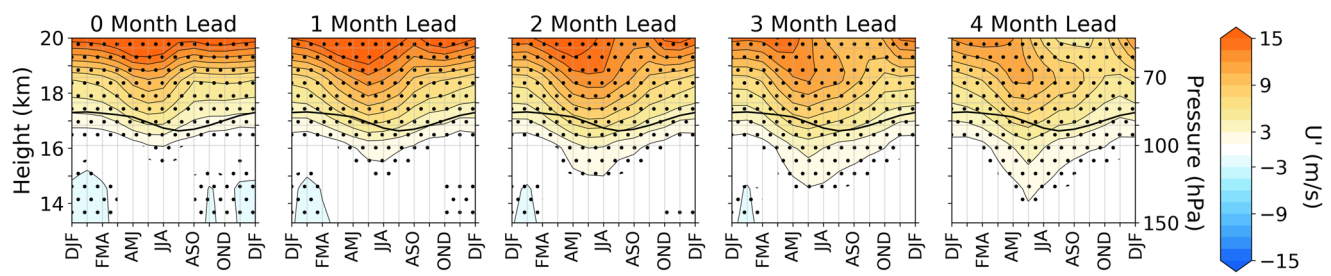

Figure 6. Seasonality of zonal-mean QBOW-QBOE anomaly composites averaged over 10°S–10°S as a function of height for zonal wind. The columns, thick black lines, and stippling are the same as in Figure 1.

opposite to those at higher levels is identified. A similar feature extending to lower levels has been found in other reanalysis data during boreal winter and spring (Gray et al., 2018; Hitchmann et al., 2021) and has been attributed to changes in the Walker circulation. This anomaly deserves more attention but is not further investigated here.

In summary, the observed seasonality of the QBO-induced cloud fraction anomalies in the tropical upper troposphere is synchronized with those of temperature, vertical temperature gradient, and zonal wind: their deep intrusions all occur in boreal spring and early summer and maximize when the QBO index at 50 hPa leads by 3 months. Assuming these intrusions are not coincidence but instead connected, we next investigate the potential drivers of this using the ERA5 reanalysis.

3.3. ERA5 Zonal Wind Tendency Analysis

Vertically extensive QBO-related signatures in cloud fraction are synchronized with tropospheric intrusions of QBO-related temperature and zonal wind (see Figures 1, 5, and 6). If these tropospheric intrusions are linked to a common physical mechanism, an investigation of the zonal wind tendencies may provide insight into what allows for these deeper intrusions in boreal spring and summer. In this section, we focus on the zonal wind signatures and attempt to document the dynamical processes that contribute to their creation and seasonality. For the QBO zonal wind signature to travel downward into the tropical upper troposphere, there must be an acceleration of the zonal mean zonal winds. Because seasonal variations in the depth of QBO zonal wind penetration were observed in Figure 6, we expect seasonal variations in the accelerations at these levels as well.

To investigate the seasonal variations of lower-stratospheric zonal wind forcings and their potential impact on the tropospheric intrusions of zonal winds, we use the transformed eulerian mean (TEM) zonal mean zonal wind tendency equation (Andrews et al., 1987).

$$\frac{\partial \overline{\boldsymbol{u}}}{\partial \boldsymbol{t}} = \frac{\mathbf{1}}{\boldsymbol{\rho_0 a \cos \phi}} \nabla \cdot \boldsymbol{F} - \overline{\boldsymbol{\omega}}^{*} \frac{\partial}{\partial \boldsymbol{z}} \left(\overline{\boldsymbol{u}}\right) - \frac{\overline{\boldsymbol{v}}^{*}}{\boldsymbol{a \cos \phi}} \frac{\partial \left(\overline{\boldsymbol{u}} \boldsymbol{\cos \phi}\right)}{\partial \boldsymbol{\phi}} + \boldsymbol{f} \overline{\boldsymbol{v}}^{*} + \boldsymbol{X} \tag{1}$$

In Equation 1, overbars represent zonal averages and asterisks denote the TEM velocity. Variable f is the Coriolis parameter, a is the radius of the Earth, $\boldsymbol{\phi}$ is the latitude, v is the meridional wind, $\boldsymbol{\omega}$ is the vertical velocity, $\boldsymbol{\rho_0}$ is the density, $\nabla \cdot \boldsymbol{F}$ denotes the divergence of Eliassen-Palm (EP) flux vectors, and $\boldsymbol{X}$ denotes the unresolved tendencies (i.e., the necessary term which closes the budget at each timestep). The term on the left-hand side of the equation can be thought of as the net acceleration seen in ERA5. The terms on the right-hand side from left to right represent accelerations arising from the EP flux divergence (divergence of eddy heat and momentum fluxes), vertical advection, horizontal advection, Coriolis force, and the residual acceleration to close the budget.

Figure 7 shows the QBO-related signal for each of the terms in Equation 1, calculated and displayed in the same way as for the anomalies previously shown in Figures 1, 5 and 6, including for different lead times of the QBO winds at 50 hPa. The first row of Figure 7 shows the QBO-related net zonal wind accelerations. At a zero-month lead, large accelerations peak around 70 hPa between late boreal winter and boreal summer, consistent with a relatively rapid descent of the QBO winds from 50 hPa in these seasons. With increasing lead time, these accelerations quickly disappear, and by a 3-month lead almost all become decelerations. These decelerations are associated with the reduction of the lower-stratospheric wind anomalies as seen in Figure 6. Note that because the acceleration is the time derivative of zonal wind, its cumulative impact on the zonal wind is its integration over time. For example, if we are interested in the zonal wind anomalies in MJJ with a 3-month lead of the QBO which penetrate into the troposphere reaching their peak, accelerations that would contribute to this impact and are observable in Figure 7 should be those from FMA with a 0-month lead, MAM with a 1-month lead, AMJ with a 2-month lead, and MJJ with a 3-month lead. The statistically significant zonal accelerations near 70 hPa and below at 0-, 1-, and 2-month leads near boreal spring may thus contribute to the below tropopause intrusions of zonal winds documented in this study.

We then look at the constituent components of the net acceleration on the right-hand side of Equation 1. The largest contribution to the net tendency comes from the EP flux divergence (second row of Figure 7). Using a zero-month QBO lead, large accelerations due to the EP flux divergence are observed from ~16 to 20 km with a large seasonal variation. Pahlavan, Wallace, et al. (2021) recently showed that a significant amount of the wave driving necessary for descent of the QBOW jet is resolved in the ERA5. Conversely, much of the easterly wind descent is tied to gravity waves that are only partly resolved in the ERA5 and would thus also show up in the

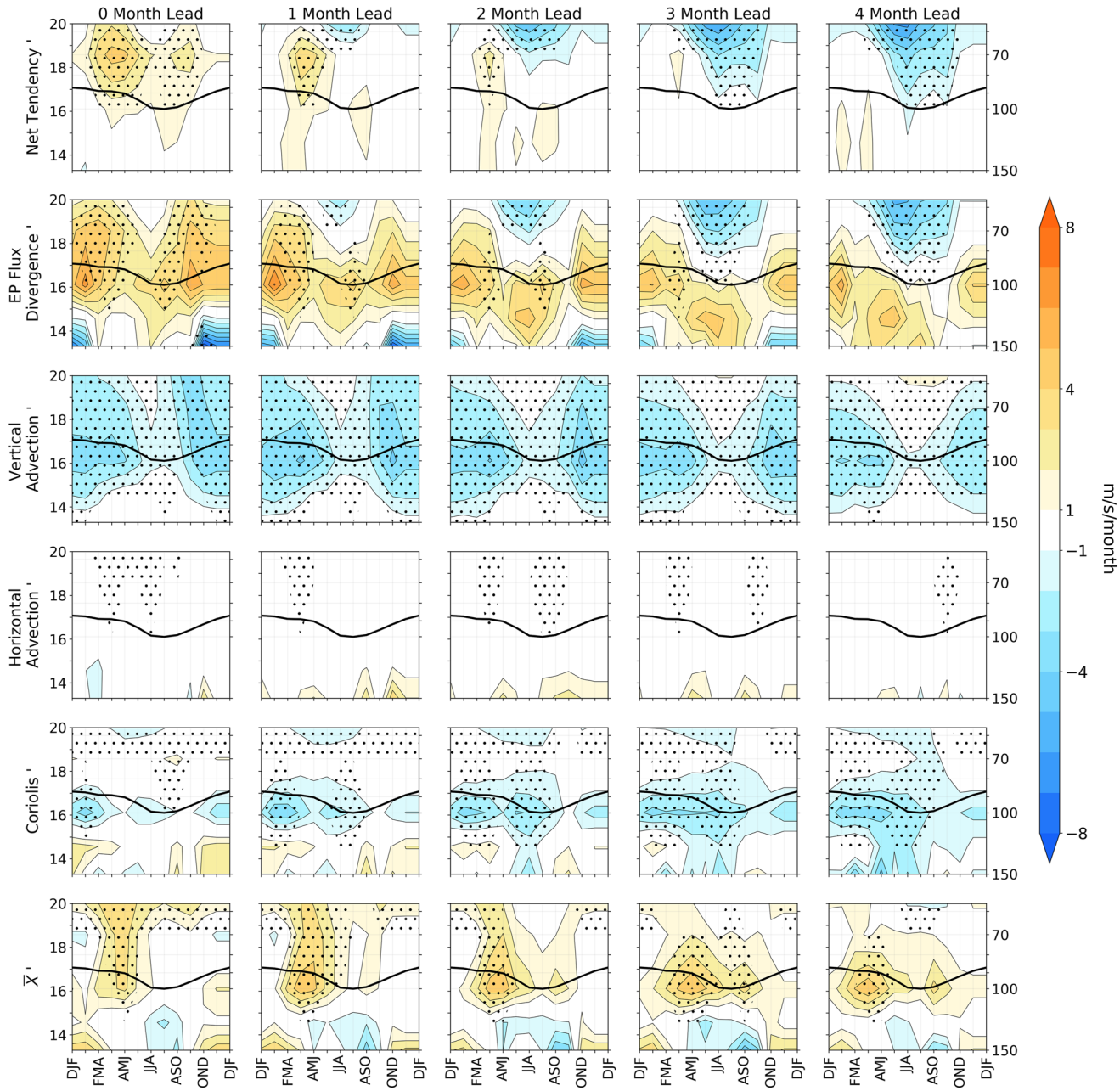

Figure 7. Seasonality of zonal-mean QBOW-QBOE accelerations averaged over 10°S–10°N as a function of height, for the net acceleration (first row), the EP flux divergence (second row), the vertical advection (third row), the horizontal advection (fourth row), the Coriolis force (fifth row) and the unresolved processes (sixth row). The columns, thick black lines, and stippling are the same as in Figure 1.

residual acceleration. The EP flux divergence also largely contributes to the breakdown of lower-stratospheric winds discussed above through the combined effects of Rossby, mixed Rossby-gravity, and Kelvin waves below about 20 km (see Figure 10 in Pahlavan, Wallace, et al., 2021). Other studies have noted seasonality in climatologies of Kelvin wave and Mixed Rossby-gravity wave activity in the TTL and lower stratosphere, with peak activity in boreal winter and spring (Maruyama, 1991; Murayama et al., 1994; Sjoberg et al., 2017; Tindall et al., 2006). Note that while the EP flux divergence is particularly large near 100 hPa in boreal winter, it is markedly smaller above the tropopause and in regions where we see positive net acceleration in the first row of Figure 6.

The second largest component of the net tendency is the vertical advection (third row of Figure 6). A strong seasonal cycle in this component is evident, which has its maximum near the tropopause in boreal winter and

minimum in boreal summer. This is consistent with the known seasonal variation of the BDC in the lower stratosphere (e.g., Rosenlof, 1995; Sevior et al., 2012). The vertical advection is related to the tropical upwelling, whereby increases in the tropical upwelling act to slow the downward propagation of the QBO (Coy et al., 2020; Hampson & Haynes, 2004; Kinnersley & Pawson, 1996; Rajendran et al., 2018; Wallace et al., 1993). Strong upwelling in boreal winter may thus inhibit the descent of the QBO into the upper troposphere (Match & Fueglistaler, 2019) whereas the weaker upwelling in late boreal spring and summer may allow for the QBO to travel further into the troposphere and contribute to the tropospheric intrusions discussed above. Because of the similar seasonality and strong cancellation in the lower stratosphere between the EP flux divergence and combined effect of the vertical advection and Coriolis torque, it is difficult to determine the primary component setting the accelerations observed in the first row of Figure 6. The fact that these processes largely cancel prohibits us from ruling out the importance of either the vertical advection or EP flux divergence in setting the seasonal cycle of tropospheric intrusions observed in this study.

The residual acceleration (sixth row of Figure 7) is contributed to by both unresolved gravity waves, and model corrections required to nudge model predictions to observations. The peak acceleration in the net tendency at 70 hPa aligns well with those in the residual acceleration, suggesting that the unresolved processes in ERA5 are important in setting the seasonal cycle of the acceleration at 70 hPa. The residual acceleration peaks in AMJ, focused mainly above the tropopause with a 0-month QBO lead, but descends with increasing lead time. Below the tropopause, the residual acceleration is strongly damped by both the vertical advection and the Coriolis force (the same is true for the EP flux divergence). The least important process identified in the tendency analysis was the horizontal advection.

4. Discussion and Summary

This study documents the seasonality of the QBO impact on equatorial high clouds using 15 years of observations from the CALIPSO satellite. When using a QBO index based on zonal wind at the 50 hPa level with a 3-month lead, significant cloud fraction responses extend down to 12.5 km, far below the region of strong QBO wind signal (>19 km). This result is similar when using QBO indices based on both 70 and 30 hPa, but with lead times of 1 and 6 months respectively, suggesting that the significance of the lead time is related to when the QBO signal would be close to the CPT. The magnitude of the QBO signal in zonal mean cloud fraction has a strong seasonal cycle, with deep intrusions only occurring during boreal spring and summer. These deep cloud fraction changes culminate with a statistically significant and independently observed change in the longwave CRE. QBO related temperature and vertical temperature gradient changes that extend from above the tropopause to near 14 km are synchronized with these vertically extensive cloud fraction changes. Measurements of these thermodynamic changes in the TTL came from GPS-RO data and are thus independent of the cloud data. QBO-related zonal winds from ERA5 were also shown to be synchronized with these cloud fraction and temperature changes. These results demonstrate a strong seasonality in the penetration depth of the QBO signal for the period considered. These results are consistent with previous studies such as Collimore et al. (2003), Tegtmeier et al. (2020), Hitchman et al. (2021), and Martin, Sobel, et al. (2021) but provide new evidence for the QBO signals in cloudiness, its vertical structure, and its coherence with other variables impacted by the QBO.

A remaining question regards the extent to which this seasonality is determined by the dynamics of the QBO within the lower stratosphere—a "top-down" effect, or by processes occurring in the troposphere—a "bottom-up" effect. Previous studies have suggested that the stratospheric QBO is influenced by the annual cycle through changes in the Semi-Annual Oscillation (Dunkerton, 1997; Dunkerton & Delisi, 1985; Kuai et al., 2009), the BDC (Coy et al., 2020; Hampson & Haynes, 2004; Rajendran et al., 2018), and the seasonality of wave-driving that reaches a given level of the atmosphere (Dunkerton, 1990; Maruyama, 1991). These would be "top-down" effects. It may also be possible that the buffer zone (Match & Fueglistaler, 2019) which determines the lower limit of the QBO, undergoes a seasonal variation making the QBO signal in the upper troposphere larger in some seasons compared to others. Further, changes in the tropical upwelling velocity associated with the BDC may impact maximum depth that the QBO can reach. If stratospheric processes set the seasonality of the tropospheric intrusions observed in this study, it may then represent an important component of stratospheric-tropospheric coupling.

Another potential mechanism by which the stratospheric QBO interacts with the tropical troposphere is through its effect on convection. In this mechanism, QBO-related temperature reductions in the upper TTL influence

the CPT and static stability (Collimore et al., 2003; Davis et al., 2013; Gray et al., 1992; Nie & Sobel, 2015). Decreased TTL temperature and static stability associated with the QBOE allow for more vigorous and frequent deep convection which cools at altitudes near the TTL (Holloway & Neelin, 2007; Tegtmeier et al., 2020), creating an even more favorable environment for convection, and starting a positive feedback loop. Similarly, increased temperatures associated with QBOW would decrease convection creating an analogous but opposite feedback. In this case, temperature and cloud fraction anomalies shown in Figures 1 and 5 influence one another and propagate the QBO signal further into the troposphere and would represent a more "bottom-up" mechanism for the seasonality of the QBO signal in the TTL and upper troposphere. Although it is not obvious why this process would lead to a seasonality as shown here these feedbacks would be more effective in seasons when convection is more active.

To analyze the potential importance of the dynamical processes in setting the seasonality of QBO impacts observed here, we used the TEM version of the zonal mean zonal wind tendency equation. We found evidence that the EP flux divergence and the vertical mean advection contribute to the seasonal cycle. This suggests that the seasonal cycles in wave-driving and the BDC are both important in setting the seasonal variations of QBO signals in the TTL. Unresolved processes were also critical in recreating the observed seasonality and would include contributions from small scale gravity waves and convective influences described in the "bottom-up" mechanism. More research is needed regarding the extent to which this seasonality is caused by a "top-down," "bottom-up," or combined mechanism.

This study also found a weak secondary minimum in zonal mean QBO-related TTL cirrus cloud fraction in DJF. This may be surprising given that the MJO, which strongly controls TTL Cirrus clouds (Hendon & Abhik, 2018; Son et al., 2017; Virts et al., 2010), was shown to have its strongest connection to the QBO in DJF. We find that much of the difference in the zonal mean cloud fraction signature between DJF and AMJ is due to longitudinal asymmetries in the cloud fraction response during DJF. Even though the zonal mean signature was weaker in DJF, TTL cirrus cloud field still shows strong responses in MJO active regions. Curiously, the AMJ cloud field also shows strong responses over MJO active regions yet there is little to no correlation between the MJO and QBO indices for this season (Son et al., 2017). It should be noted that cloud fraction changes shown here are seasonal mean changes, and thus are not entirely comparable to those related to the MJO In total, the DJF local minimum in zonal mean clouds should not be taken as evidence contrary to hypotheses linking the QBO and MJO through cirrus. Instead, results in this study lead to a different question: If cirrus clouds are important to linking the QBO and MJO, why is there little connection during other seasons when the QBO related cirrus response is strong both in the zonal mean and over the MJO active longitudes?

In conclusion, this study shows that QBO-related changes in the equatorial high cloud fields can extend from tropopause to ∼12 km and induce significant changes in the longwave CRE. These changes in cloud fraction are largely confined to boreal spring and summer and are synchronized with changes in temperature, vertical temperature gradient, and zonal wind in the TTL. Clouds and temperature are linked through convective and radiative effects, whereas temperature and zonal winds are linked through thermal wind balance, thus causal directions are difficult to decipher in this study. By noting that the data only span 15 years and thus only contain ∼6 QBO cycles, longer data records would be useful to confirm results of this study. We found based on the ERA5 reanalysis that the seasonality of the zonal wind response to the QBO for 1979–2020 is very similar to that of 2006–2020 (not shown). This study suggests that using the zonal mean equatorial region can provide perspective on the QBO direct impact on the troposphere. Critical to observing this connection is looking in boreal spring and summer when the connection is strongest. An important remaining question is what sets the seasonality of the QBO impact on the TTL.

Conflict of Interest

The authors declare no conflicts of interest relevant to this study.

Data Availability Statement

The code used to create this work is publicly available on Aodhan Sweeney's GitHub account (https://github.com/AodhanSweeney/QBOSeasonality2023). Code and processed versions of the data required to recreate results are held on a dedicated zenodo page with https://doi.org/10.5281/zenodo.7502019.

Acknowledgments
This research is supported by the NASA FINESST Grant 80NSSC22K1438 and NSF Grant AGS-2202812. Q.F.'s visit to the University of Cambridge is partly supported by the Leverhulme Visiting Professorship.

References

Andrews, D. G., Holton, J. R., & Leovy, C. B. (1987). Middle atmosphere dynamics. https://www.osti.gov/biblio/5936274

Anstey, J. A., & Shepherd, T. G. (2014). High-latitude influence of the Quasi-Biennial oscillation. *Quarterly Journal of the Royal Meteorological Society*, *140*(678), 1–21. https://doi.org/10.1002/qj.2132

Baldwin, M. P., Gray, L. J., Dunkerton, T. J., Hamilton, K., Haynes, P. H., Randel, W. J., et al. (2001). The Quasi-Biennial Oscillation. *Reviews of Geophysics*, *39*(2), 179–229. https://doi.org/10.1029/1999RG000073

Chang, K.-W., & L'Ecuyer, T. (2020). Influence of gravity wave temperature anomalies and their vertical gradients on cirrus clouds in the tropical tropopause layer—A satellite-based view. *Atmospheric Chemistry and Physics*, *20*(21), 12499–12514. https://doi.org/10.5194/acp-20-12499-2020

Collimore, C. C., Martin, D. W., Hitchman, M. H., Huesmann, A., & Waliser, D. E. (2003). On the relationship between the QBO and tropical deep convection. *Journal of Climate*, *16*(15), 2552–2568. https://doi.org/10.1175/1520-0442(2003)016<2552:OTRBTQ>2.0.CO;2

Corti, T., Luo, B. P., Fu, Q., Vömel, H., & Peter, T. (2006). The impact of cirrus clouds on tropical troposphere-to-stratosphere transport. *Atmospheric Chemistry and Physics*, *6*(9), 2539–2547. https://doi.org/10.5194/acp-6-2539-2006

Corti, T., Luo, B. P., Peter, T., Vömel, H., & Fu, Q. (2005). Mean radiative energy balance and vertical mass fluxes in the equatorial upper troposphere and lower stratosphere. *Geophysical Research Letters*, *32*(6), L06802. https://doi.org/10.1029/2004GL021889

Coy, L., Newman, P. A., Strahan, S., & Pawson, S. (2020). Seasonal variation of the quasi-biennial oscillation descent. *Journal of Geophysical Research: Atmospheres*, *125*(18), e2020JD033077. https://doi.org/10.1029/2020JD033077

Davis, S. M., Liang, C. K., & Rosenlof, K. H. (2013). Interannual variability of tropical tropopause layer clouds. *Geophysical Research Letters*, *40*(11), 2862–2866. https://doi.org/10.1002/grl.50512

Densmore, C. R., Sanabia, E. R., & Barrett, B. S. (2019). QBO influence on MJO amplitude over the maritime continent: Physical mechanisms and seasonality. *Monthly Weather Review*, *147*(1), 389–406. https://doi.org/10.1175/MWR-D-18-0158.1

Dessler, A. E., Schoeberl, M. R., Wang, T., Davis, S. M., & Rosenlof, K. H. (2013). Stratospheric water vapor feedback. *Proceedings of the National Academy of Sciences of the United States of America*, *110*(45), 18087–18091. https://doi.org/10.1073/pnas.1310344110

Ding, Q., & Fu, Q. (2018). A warming tropical central Pacific dries the lower stratosphere. *Climate Dynamics*, *50*(7), 2813–2827. https://doi.org/10.1007/s00382-017-3774-y

Dunkerton, T. (1990). Annual variation of deseasonalized mean flow acceleration in the equatorial lower stratosphere. https://doi.org/10.2151/JMSJ1965.68.4_499

Dunkerton, T. J. (1997). The role of gravity waves in the Quasi-Biennial Oscillation. *Journal of Geophysical Research*, *102*(D22), 26053–26076. https://doi.org/10.1029/96JD02999

Dunkerton, T. J., & Delisi, D. P. (1985). Climatology of the equatorial lower stratosphere. *Journal of the Atmospheric Sciences*, *42*(4), 376–396. https://doi.org/10.1175/1520-0469(1985)042<0376:COTELS>2.0.CO;2

Flury, T., Wu, D. L., & Read, W. G. (2012). Correlation among cirrus ice content, water vapor and temperature in the TTL as observed by CALIPSO and Aura/MLS. *Atmospheric Chemistry and Physics*, *12*(2), 683–691. https://doi.org/10.5194/acp-12-683-2012

Fu, Q., Hu, Y., & Yang, Q. (2007). Identifying the top of the tropical tropopause layer from vertical mass flux analysis and CALIPSO lidar cloud observations. *Geophysical Research Letters*, *34*(14), L14813. https://doi.org/10.1029/2007GL030099

Fu, Q., Smith, M., & Yang, Q. (2018). The impact of cloud radiative effects on the tropical tropopause layer temperatures. *Atmosphere*, *9*(10), 377. https://doi.org/10.3390/atmos9100377

Fueglistaler, S., Dessler, A. E., Dunkerton, T. J., Folkins, I., Fu, Q., & Mote, P. W. (2009). Tropical tropopause layer. *Reviews of Geophysics*, *47*(1). https://doi.org/10.1029/2008RG000267

Fueglistaler, S., & Fu, Q. (2006). Impact of clouds on radiative heating rates in the tropical lower stratosphere. *Journal of Geophysical Research*, *111*(D23), D23202. https://doi.org/10.1029/2006JD007273

Fueglistaler, S., & Haynes, P. H. (2005). Control of interannual and longer-term variability of stratospheric water vapor. *Journal of Geophysical Research*, *110*(D24), D24108. https://doi.org/10.1029/2005JD006019

García-Franco, J. L., Gray, L. J., Osprey, S., Chadwick, R., & Martin, Z. (2022). The tropical route of quasi-biennial oscillation (QBO) teleconnections in a climate model. *Weather and Climate Dynamics*, *3*(3), 825–844. https://doi.org/10.5194/wcd-3-825-2022

Giorgetta, M. A., Bengtsson, L., & Arpe, K. (1999). An investigation of QBO signals in the east Asian and Indian monsoon in GCM experiments. *Climate Dynamics*, *15*(6), 435–450. https://doi.org/10.1007/s003820050292

Gray, L. J., Anstey, J. A., Kawatani, Y., Lu, H., Osprey, S., & Schenzinger, V. (2018). Surface impacts of the Quasi Biennial Oscillation. *Atmospheric Chemistry and Physics*, *18*(11), 8227–8247. https://doi.org/10.5194/acp-18-8227-2018

Gray, W. M., Sheaffer, J. D., & Knaff, J. A. (1992). Influence of the stratospheric QBO on ENSO variability. *Journal of the Meteorological Society of Japan. Series II*, *70*(5), 975–995. https://doi.org/10.2151/jmsj1965.70.5_975

Hampson, J., & Haynes, P. (2004). Phase alignment of the tropical stratospheric QBO in the annual cycle. *Journal of the Atmospheric Sciences*, *61*(21), 2627–2637. https://doi.org/10.1175/JAS3276.1

Hartmann, D. L., Holton, J. R., & Fu, Q. (2001). The heat balance of the tropical tropopause, cirrus, and stratospheric dehydration. *Geophysical Research Letters*, *28*(10), 1969–1972. https://doi.org/10.1029/2000GL012833

Haynes, P., Hitchcock, P., Hitchman, M., Yoden, S., Hendon, H., Kiladis, G., et al. (2021). The influence of the stratosphere on the tropical troposphere. *Journal of the Meteorological Society of Japan. Series II*, *99*(4), 803–845. https://doi.org/10.2151/jmsj.2021-040

Hendon, H. H., & Abhik, S. (2018). Differences in vertical structure of the Madden-Julian oscillation associated with the Quasi-Biennial oscillation. *Geophysical Research Letters*, *45*(9), 4419–4428. https://doi.org/10.1029/2018GL077207

Hersbach, H., Bell, B., Berrisford, P., Hirahara, S., Horányi, A., Muñoz-Sabater, J., et al. (2020). The ERA5 global reanalysis. *Quarterly Journal of the Royal Meteorological Society*, *146*(730), 1999–2049. https://doi.org/10.1002/qj.3803

Hitchman, M. H., Yoden, S., Haynes, P. H., Kumar, V., & Tegtmeier, S. (2021). An observational history of the direct influence of the stratospheric Quasi-Biennial oscillation on the tropical and subtropical upper troposphere and lower stratosphere. *Journal of the Meteorological Society of Japan. Series II*, *99*(2), 239–267. https://doi.org/10.2151/jmsj.2021-012

Holloway, C. E., & Neelin, J. D. (2007). The convective cold top and quasi equilibrium. *Journal of the Atmospheric Sciences*, *64*(5), 1467–1487. https://doi.org/10.1175/JAS3907.1

Holton, J. R., & Lindzen, R. S. (1972). An updated theory for the quasi-biennial cycle of the tropical stratosphere. *Journal of the Atmospheric Sciences*, *29*(6), 1076–1080. https://doi.org/10.1175/1520-0469(1972)029<1076:AUTFTQ>2.0.CO;2

Holton, J. R., & Tan, H.-C. (1980). The influence of the equatorial quasi-biennial oscillation on the global circulation at 50 mb. *Journal of the Atmospheric Sciences*, *37*(10), 2200–2208. https://doi.org/10.1175/1520-0469(1980)037<2200:TIOTEQ>2.0.CO;2

Holton, J. R., & Tan, H.-C. (1982). The Quasi-Biennial oscillation in the northern hemisphere lower stratosphere. *Journal of the Meteorological Society of Japan. Series II*, *60*(1), 140–148. https://doi.org/10.2151/jmsj1965.60.1_140
Hong, Y., Liu, G., & Li, J.-L. F. (2016). Assessing the radiative effects of global ice clouds based on CloudSat and CALIPSO Measurements. *Journal of Climate*, *29*(21), 7651–7674. https://doi.org/10.1175/JCLI-D-15-0799.1
Huesmann, A. S., & Hitchman, M. H. (2001). The stratospheric Quasi-Biennial oscillation in the NCEP reanalyses: Climatological structures. *Journal of Geophysical Research*, *106*(D11), 11859–11874. https://doi.org/10.1029/2001JD900031
Jaramillo, A., Dominguez, C., Raga, G., & Quintanar, A. I. (2021). The combined QBO and ENSO influence on tropical cyclone activity over the North Atlantic Ocean. *Atmosphere*, *12*(12), 1588. Article 12. https://doi.org/10.3390/atmos12121588
Kim, J.-E., Alexander, M. J., Bui, T. P., Dean-Day, J. M., Lawson, R. P., Woods, S., et al. (2016). Ubiquitous influence of waves on tropical high cirrus clouds. *Geophysical Research Letters*, *43*(11), 5895–5901. https://doi.org/10.1002/2016GL069293
Kinnersley, J. S., & Pawson, S. (1996). The descent rates of the shear zones of the equatorial QBO. *Journal of the Atmospheric Sciences*, *53*(14), 1937–1949. https://doi.org/10.1175/1520-0469(1996)053<1937:TDROTS>2.0.CO;2
Klotzbach, P., Abhik, S., Hendon, H. H., Bell, M., Lucas, C., Marshall, A., & Oliver, E. C. J. (2019). On the emerging relationship between the stratospheric Quasi-Biennial oscillation and the Madden-Julian oscillation. *Scientific Reports*, *9*(1), 2981. https://doi.org/10.1038/s41598-019-40034-6
Krismer, T. R., Giorgetta, M. A., & Esch, M. (2013). Seasonal aspects of the quasi-biennial oscillation in the max Planck Institute Earth System Model and ERA-40. *Journal of Advances in Modeling Earth Systems*, *5*(2), 406–421. https://doi.org/10.1002/jame.20024
Kuai, L., Shia, R.-L., Jiang, X., Tung, K.-K., & Yung, Y. L. (2009). Nonstationary synchronization of equatorial QBO with SAO in observations and a model. *Journal of the Atmospheric Sciences*, *66*(6), 1654–1664. https://doi.org/10.1175/2008JAS2857.1
Kuo, Y.-H., Wee, T.-K., Sokolovskiy, S., Rocken, C., Schreiner, W., Hunt, D., & Anthes, R. A. (2004). Inversion and error estimation of GPS radio occultation data. *Journal of the Meteorological Society of Japan. Series II*, *82*(1B), 507–531. https://doi.org/10.2151/jmsj.2004.507
Kursinski, E. R., Hajj, G. A., Schofield, J. T., Linfield, R. P., & Hardy, K. R. (1997). Observing Earth's atmosphere with radio occultation measurements using the Global Positioning System. *Journal of Geophysical Research*, *102*(D19), 23429–23465. https://doi.org/10.1029/97JD01569
Lane, T. P. (2021). Does lower-stratospheric shear influence the mesoscale organization of convection? *Geophysical Research Letters*, *48*(3), e2020GL091025. https://doi.org/10.1029/2020GL091025
Liess, S., & Geller, M. A. (2012). On the relationship between QBO and distribution of tropical deep convection. *Journal of Geophysical Research*, *117*(D3), D03108. https://doi.org/10.1029/2011JD016317
Lim, Y., & Son, S.-W. (2022). QBO wind influence on MJO-induced temperature anomalies in the upper troposphere and lower stratosphere in an idealized model. *Journal of the Atmospheric Sciences*, *79*(9), 2219–2228. https://doi.org/10.1175/JAS-D-21-0296.1
Lin, J., & Emanuel, K. (2022). Stratospheric modulation of the MJO through cirrus cloud feedbacks. https://doi.org/10.48550/arXiv.2204.02379
Lindzen, R. S., & Holton, J. R. (1968). A theory of the Quasi-Biennial oscillation. *Journal of the Atmospheric Sciences*, *25*(6), 1095–1107. https://doi.org/10.1175/1520-0469(1968)025<1095:ATOTQB>2.0.CO;2
Loeb, N. G., Doelling, D. R., Wang, H., Su, W., Nguyen, C., Corbett, J. G., et al. (2018). Clouds and the Earth's radiant energy System (CERES) energy balanced and filled (EBAF) top-of-atmosphere (TOA) edition-4.0 data product. *Journal of Climate*, *31*(2), 895–918. https://doi.org/10.1175/JCLI-D-17-0208.1
Lu, H., Hitchman, M. H., Gray, L. J., Anstey, J. A., & Osprey, S. M. (2020). On the role of Rossby wave breaking in the quasi-biennial modulation of the stratospheric polar vortex during boreal winter. *Quarterly Journal of the Royal Meteorological Society*, *146*(729), 1939–1959. https://doi.org/10.1002/qj.3775
Martin, Z., Sobel, A., Butler, A., & Wang, S. (2021). Variability in QBO temperature anomalies on annual and decadal time scales. *Journal of Climate*, *34*(2), 589–605. https://doi.org/10.1175/JCLI-D-20-0287.1
Martin, Z., Son, S.-W., Butler, A., Hendon, H., Kim, H., Sobel, A., et al. (2021). The influence of the Quasi-Biennial oscillation on the Madden–Julian oscillation. *Nature Reviews Earth & Environment*, *2*(7), 477–489. https://doi.org/10.1038/s43017-021-00173-9
Martin, Z., Wang, S., Nie, J., & Sobel, A. (2019). The impact of the QBO on MJO convection in cloud-resolving simulations. *Journal of the Atmospheric Sciences*, *76*(3), 669–688. https://doi.org/10.1175/JAS-D-18-0179.1
Maruyama, T. (1991). Annual and QBO-synchronized variations of lower-stratospheric equatorial wave activity over Singapore during 1961–1989. *Journal of the Meteorological Society of Japan. Series II*, *69*(2), 219–232. https://doi.org/10.2151/jmsj1965.69.2_219
Match, A., & Fueglistaler, S. (2019). The buffer zone of the quasi-biennial oscillation. *Journal of the Atmospheric Sciences*, *76*(11), 3553–3567. https://doi.org/10.1175/JAS-D-19-0151.1
Mote, P. W., Rosenlof, K. H., McIntyre, M. E., Carr, E. S., Gille, J. C., Holton, J. R., et al. (1996). An atmospheric tape recorder: The imprint of tropical tropopause temperatures on stratospheric water vapor. *Journal of Geophysical Research*, *101*(D2), 3989–4006. https://doi.org/10.1029/95JD03422
Murayama, Y., Tsuda, T., & Fukao, S. (1994). Seasonal variation of gravity wave activity in the lower atmosphere observed with the MU radar. *Journal of Geophysical Research*, *99*(D11), 23057–23069. https://doi.org/10.1029/94JD01717
Nie, J., & Sobel, A. H. (2015). Responses of tropical deep convection to the QBO: Cloud-resolving simulations. *Journal of the Atmospheric Sciences*, *72*(9), 3625–3638. https://doi.org/10.1175/JAS-D-15-0035.1
Pahlavan, H. A., Fu, Q., Wallace, J. M., & Kiladis, G. N. (2021). Revisiting the quasi-biennial oscillation as seen in ERA5. Part I: Description and momentum budget. *Journal of the Atmospheric Sciences*, *78*(3), 673–691. https://doi.org/10.1175/JAS-D-20-0248.1
Pahlavan, H. A., Wallace, J. M., Fu, Q., & Kiladis, G. N. (2021). Revisiting the quasi-biennial oscillation as seen in ERA5. Part II: Evaluation of waves and wave forcing. *Journal of the Atmospheric Sciences*, *78*(3), 693–707. https://doi.org/10.1175/JAS-D-20-0249.1
Plumb, R. A., & Bell, R. C. (1982). A model of the quasi-biennial oscillation on an equatorial beta-plane. *Quarterly Journal of the Royal Meteorological Society*, *108*(456), 335–352. https://doi.org/10.1002/qj.49710845604
Rajendran, K., Moroz, I. M., Osprey, S. M., & Read, P. L. (2018). Descent rate models of the synchronization of the quasi-biennial oscillation by the annual cycle in tropical upwelling. *Journal of the Atmospheric Sciences*, *75*(7), 2281–2297. https://doi.org/10.1175/JAS-D-17-0267.1
Rosenlof, K. H. (1995). Seasonal cycle of the residual mean meridional circulation in the stratosphere. *Journal of Geophysical Research*, *100*(D3), 5173–5191. https://doi.org/10.1029/94JD03122
Sakaeda, N., Dias, J., & Kiladis, G. N. (2020). The unique characteristics and potential mechanisms of the MJO-QBO relationship. *Journal of Geophysical Research: Atmospheres*, *125*(17), e2020JD033196. https://doi.org/10.1029/2020JD033196
Saravanan, R. (1990). A multiwave model of the quasi-biennial oscillation. *Journal of the Atmospheric Sciences*, *47*(21), 2465–2474. https://doi.org/10.1175/1520-0469(1990)047<2465:AMMOTQ>2.0.CO;2
Seviour, W. J. M., Butchart, N., & Hardiman, S. C. (2012). The Brewer–Dobson circulation inferred from ERA-Interim. *Quarterly Journal of the Royal Meteorological Society*, *138*(665), 878–888. https://doi.org/10.1002/qj.966

Sjoberg, J. P., Birner, T., & Johnson, R. H. (2017). Intraseasonal to interannual variability of Kelvin wave momentum fluxes as derived from high-resolution radiosonde data. *Atmospheric Chemistry and Physics*, *17*(14), 8971–8986. https://doi.org/10.5194/acp-17-8971-2017

Sokol, A. B., & Hartmann, D. L. (2020). Tropical anvil clouds: Radiative driving toward a preferred state. *Journal of Geophysical Research: Atmospheres*, *125*(21), e2020JD033107. https://doi.org/10.1029/2020JD033107

Son, S.-W., Lim, Y., Yoo, C., Hendon, H. H., & Kim, J. (2017). Stratospheric control of the Madden–Julian oscillation. *Journal of Climate*, *30*(6), 1909–1922. https://doi.org/10.1175/JCLI-D-16-0620.1

Sweeney, A. J., & Fu, Q. (2021). Diurnal cycles of synthetic microwave sounding lower-stratospheric temperatures from radio occultation observations, reanalysis, and model simulations. *Journal of Atmospheric and Oceanic Technology*, *38*(12), 2045–2059. https://doi.org/10.1175/JTECH-D-21-0071.1

Tegtmeier, S., Anstey, J., Davis, S., Ivanciu, I., Jia, Y., McPhee, D., & Pilch Kedzierski, R. (2020). Zonal asymmetry of the QBO temperature signal in the tropical tropopause region. *Geophysical Research Letters*, *47*(24), e2020GL089533. https://doi.org/10.1029/2020GL089533

Tindall, J. C., Thuburn, J., & Highwood, E. J. (2006). Equatorial waves in the lower stratosphere. II: Annual and interannual variability. *Quarterly Journal of the Royal Meteorological Society*, *132*(614), 195–212. https://doi.org/10.1256/qj.04.153

Tseng, H.-H., & Fu, Q. (2017a). Temperature control of the variability of tropical tropopause layer cirrus clouds. *Journal of Geophysical Research: Atmospheres*, *122*(20), 11062–11075. https://doi.org/10.1002/2017JD027093

Tseng, H.-H., & Fu, Q. (2017b). Tropical tropopause layer cirrus and its relation to tropopause. *Journal of Quantitative Spectroscopy and Radiative Transfer*, *188*, 118–131. https://doi.org/10.1016/j.jqsrt.2016.05.029

Virts, K. S., & Wallace, J. M. (2014). Observations of temperature, wind, cirrus, and trace gases in the tropical tropopause transition layer during the MJO. *Journal of the Atmospheric Sciences*, *71*(3), 1143–1157. https://doi.org/10.1175/JAS-D-13-0178.1

Virts, K. S., Wallace, J. M., Fu, Q., & Ackerman, T. P. (2010). Tropical tropopause transition layer cirrus as represented by CALIPSO lidar observations. *Journal of the Atmospheric Sciences*, *67*(10), 3113–3129. https://doi.org/10.1175/2010JAS3412.1

Wallace, J. M., Panetta, R. L., & Estberg, J. (1993). Representation of the equatorial stratospheric quasi-biennial oscillation in EOF phase space. *Journal of the Atmospheric Sciences*, *50*(12), 1751–1762. https://doi.org/10.1175/1520-0469(1993)050<1751:ROTESQ>2.0.CO;2

Wang, M., & Fu, Q. (2021). Stratosphere-troposphere exchange of air masses and ozone concentrations based on reanalyzes and observations. *Journal of Geophysical Research: Atmospheres*, *126*(18), e2021JD035159. https://doi.org/10.1029/2021JD035159

Winker, D. M., Pelon, J., Coakley, J. A., Ackerman, S. A., Charlson, R. J., Colarco, P. R., et al. (2010). The CALIPSO mission: A global 3D view of aerosols and clouds. *Bulletin of the American Meteorological Society*, *91*(9), 1211–1230. https://doi.org/10.1175/2010BAMS3009.1

Yamazaki, K., Nakamura, T., Ukita, J., & Hoshi, K. (2020). A tropospheric pathway of the stratospheric Quasi-Biennial oscillation (QBO) impact on the boreal winter polar vortex. *Atmospheric Chemistry and Physics*, *20*(8), 5111–5127. https://doi.org/10.5194/acp-20-5111-2020

Yang, Q., Fu, Q., & Hu, Y. (2010). Radiative impacts of clouds in the tropical tropopause layer. *Journal of Geophysical Research*, *115*(D4), D00H12. https://doi.org/10.1029/2009JD012393

Yoo, C., & Son, S.-W. (2016). Modulation of the boreal wintertime Madden-Julian oscillation by the stratospheric Quasi-Biennial oscillation. *Geophysical Research Letters*, *43*(3), 1392–1398. https://doi.org/10.1002/2016GL067762

Zeng, Z., Sokolovskiy, S., Schreiner, W. S., & Hunt, D. (2019). Representation of vertical atmospheric structures by radio occultation observations in the upper troposphere and lower stratosphere: Comparison to high-resolution radiosonde profiles. *Journal of Atmospheric and Oceanic Technology*, *36*(4), 655–670. https://doi.org/10.1175/JTECH-D-18-0105.1

Zhang, C., & Zhang, B. (2018). QBO-MJO connection. *Journal of Geophysical Research: Atmospheres*, *123*(6), 2957–2967. https://doi.org/10.1002/2017JD028171